energies

MDPI

Article

Sustainable Corrosion Inhibitors from Pharmaceutical Wastes: Advancing Energy-Efficient Chemistry with Green Solutions

Narasimha Raghavendra [1], Sharanappa Chapi [2,*], Murugendrappa M. V. [2], Małgorzata Pawlak [3,*] and Mohammad Reza Saeb [4]

[1] Department of Chemistry, K. L. E. Society's P. C. Jabin Science College, Hubballi 580031, Karnataka, India; rcbhat3@gmail.com
[2] Department of Physics, B. M. S. College of Engineering, Bull Temple Road, Basavanagudi, Bengaluru 560019, Karnataka, India; murugendrappamv.phy@bmsce.ac.in
[3] Department of Ship Operation, Faculty of Navigation, Gdynia Maritime University, 81-87 Morska St., 81-225 Gdynia, Poland
[4] Department of Pharmaceutical Chemistry, Medical University of Gdańsk, J. Hallera 107, 80-416 Gdańsk, Poland; mr.saeb@gumed.edu.pl
* Correspondence: sharanappac.phy@bmsce.ac.in (S.C.); m.pawlak@wn.umg.edu.pl (M.P.)

Abstract: Pharmaceutical waste is a type of bio-waste inevitably generated by the pharmaceutical industry, often due to regulatory changes, product deterioration, or expiration. However, their collection and valorization can be approached from a sustainable perspective, offering potential energy-efficient solutions. In this work, the expired Eslicarbazepine acetate drug (ESLD) was utilized as a sustainable anticorrosive agent against mild steel in a 3 M HCl wash solution. Experimental tests combined with theoretical Density Functional Theory (DFT) and Monte Carlo (MC) simulations revealed the corrosion inhibition potential of ESLD. The gasometrical results revealed a high inhibition efficiency rate of 98% upon increases in concentration of expired ESLD from 0.25 to 1.00 mg·L^{-1}, whereas hydrogen gas evolution decreased to 0.7 mL. An impedance investigation evidenced the pivotal role of charge transfer in reducing the disintegration process. As per DFT computations and MC simulation, electron-rich elements in the expired ESLD were key in controlling the dissolution through the adsorption process. Contact angle studies revealed that the increment in the contact angle from 61° to 80° in the presence of expired ESLD validates the chemical, electrochemical, and computational results. This approach not only mitigates pharmaceutical pollution, but also exemplifies the integration of green chemistry principles into corrosion protection, contributing to energy-efficient and sustainable industrial practices.

Keywords: pharmaceutical materials; Monte Carlo simulation; DFT computation; contact angle; corrosion inhibitor

check for updates

Academic Editor: Byong-Hun Jeon

Received: 25 November 2024
Revised: 28 December 2024
Accepted: 3 January 2025
Published: 7 January 2025

Citation: Raghavendra, N.; Chapi, S.; M. V., M.; Pawlak, M.; Saeb, M.R. Sustainable Corrosion Inhibitors from Pharmaceutical Wastes: Advancing Energy-Efficient Chemistry with Green Solutions. *Energies* **2025**, *18*, 224. https://doi.org/10.3390/en18020224

Copyright: © 2025 by the authors. Licensee MDPI, Basel, Switzerland. This article is an open access article distributed under the terms and conditions of the Creative Commons Attribution (CC BY) license (https://creativecommons.org/licenses/by/4.0/).

1. Introduction

Pharmaceutical wastes are significant environmental pollutants found in soil and water. However, expired drugs are generally less toxic and can be converted in situ into valuable agents. Given that drugs and pharmaceuticals are bio-based, thoughtful conversion of such wastes can lead to the development of sustainable agents with desirable properties, while also promoting environmental friendliness. In this context, a variety of applications can be explored based on the chemical composition and functionality of expired drugs. Mild steel (MS) is considered a superior-performance industrial unit material in various industrial sections. It is a widely used material in many industries, but it is prone to corrosion in various corrosive environments. Among numerous commercial acids,

HCl is broadly utilized in various industrial applications. In industrial processes, HCl is typically used to remove unwanted scale and rust [1]. This is largely employed for the etching, descaling, cleaning, and pickling of MS, which causes the metal to corrode [2–4]. This results in major protection concerns and substantial economic losses [5–8]. Therefore, there has always been a strong and important need for highly efficient corrosion inhibitors [9]. Using organic compounds as corrosion inhibitors is now thought to be the most effective way to stop the disintegration of metal [10–12]. It is anticipated that a variety of organic compounds with various functional moieties will exhibit strong corrosion inhibition capabilities. Nevertheless, understanding molecular- and atomic-level mechanisms undertaking corrosion inhibition phenomena under various conditions and media has also been considered a supplement to experimental analyses [13,14].

The effectiveness of organic compounds as corrosion inhibitors primarily relies on their ability to adsorb onto the metal surface via dynamic sites like π bonds, heteroatoms (O, S, and N), and polar functional moieties [15,16]. These species create invisible barrier films on the metal surface by chemical adsorption (covalent bonds) or physical adsorption (electrostatic interaction), which protects the metal from corrosive attack. According to the literature, the majority of organic species displace water molecules and form a barrier layer as they are adsorbed over the metal surface [17]. Organic compounds have a lone pair of electrons and pi bonds, which help transfer electrons from the corrosion inhibitor to the metal surface and form a coordinated covalent bond [18]. The strength of the chemical adsorption mainly depends on the polarizability group and donor atom of the functional group. However, most of the organic compounds are toxic to high degrees to human beings and the environment. Therefore, the development of zero- or low-toxicity corrosion inhibitors is very desirable and essential to both academia and industries alike [19].

Medicinal compounds and biomaterial waste generally contain heterocyclic rings, and benzene exhibits environmental properties that can replace the toxic organic corrosion inhibitors [20,21]. There have been some reports on the use of expired pharmaceuticals and drugs as corrosion inhibitors, analyzing their anticorrosive efficiency towards MS [22], but, meanwhile, the challenges of the poor stability of expired drugs have also been outlined [23]. However, no reports have been found on the use of expired eslicarbazepine acetate (ESLD) as a sustainable corrosion inhibitor, which underscores the need for this research. From a healthcare perspective, two factors should be considered when using expired ESLD as a corrosion inhibitor. First, to the best of the authors' knowledge, there are no explicit data on the toxicity of expired ESLD and its potential impact on both the environment and human health. Second, corrosion inhibitors are typically added to thermosetting materials along with other ingredients and then crosslinked, which significantly reduces the possibility of ingredient diffusion through the crosslinked structure. Actually, there is no toxicity, and it is able to inhibit corrosion.

The chemical structure of the expired ESLD drug, together with atomic bonds, is depicted in Figure 1. The presence of both amine and oxygen as well as ester in its structure makes ESLD highly reactive. This work for the first-time reports on the anticorrosive and corrosion inhibition potential of ESLD within a 3 M HCl solution. The experimental investigations, including gasometric and electrochemical (potentiodynamic polarization and impedance) analyses, contact angle and scanning electron microscopy (SEM), and surface characteristics of MS affected by ESLD application, are monitored. The computational analyses using Density Functional Theory (DFT) and Monte Carlo (MC) simulation were combined with experiments to explore ESLD interactions in terms of electron donation.

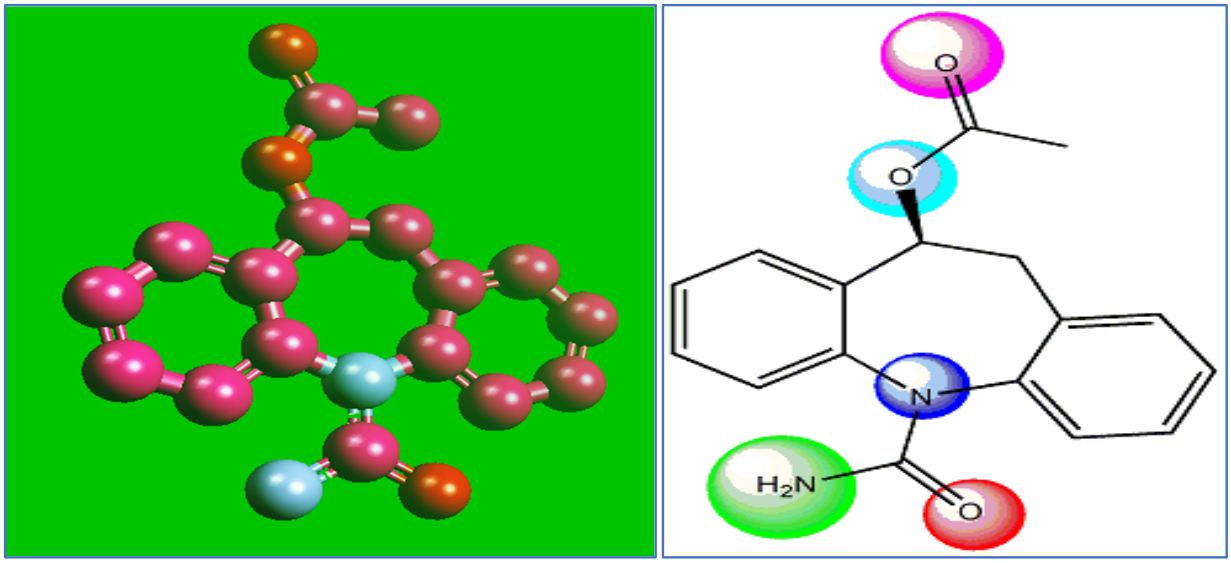


Figure 1. Interactive chemical structure model (Ball and Stick) and chemical structure depiction of ESLD.

2. Materials and Methods

Mild steel (MS: Fe 99.03%) purchased from Sri Durga Lab Equipment Supplies—Mangalore, India. The MS elemental composition used in the present investigation was Si-0.1, S-0.05, P-0.04, C-0.18, and Mn-0.6 [24]. MS pieces with an exposed surface area of 1 cm^2 were used for the electrochemical and SEM investigations. The specimens were thoroughly cleaned before usage, and the exposed region was mechanically abraded using various emery paper grades, cleaned with water and acetone, dried, and desiccated for additional research. A 3 M aqueous HCl was prepared as a corrosive solution (bare system) on MS by diluting the concentrated HCl solution. Four different concentrations (0.25, 0.5, 0.75, and 1 mg/L) of expired ESLD were added to the bare system. An electrochemical test was performed by using an electrochemical analyzer (CHI660C, CH Instrument, Austin, TX, USA) consisting of three electrodes (Platinum counter electrode, Calomel reference electrode, and MS working electrode). Prior to each measurement, the MD was exposed to 3 M HCl at the Open Circuit Potential (OCP) for 40 min. AC impedance spectroscopy was performed at an amplitude of 5 mV in the frequency range of 10^5 to 10^{-3} Hz. Potentiodynamic polarization curves were obtained within a potential range of ±250 mV at 10^{-2} V/s. A 100 mL solution of 3 M HCl was used for the gasometric experiment with and without an expired ESLD. The gasometric apparatus contained a reaction vessel and the burette evaluated the hydrogen gas evolution from the corrosive reaction [25]. The air volume (from the burette) was observed with exposure periods of 2, 4, 6, 8, 10, and 12 h. DFT studies were performed by using Gaussian 3 software (Gaussian 03). MC simulation was used to gain a better understanding of the adsorption of the expired ESLD on the MS surface (1 1 0) in an aqueous environment. BIOVIA Materials Studio -2023 (Dassault Systèmes) and an adsorption locator were utilized for the simulation. The various parameters obtained from computational studies are discussed here in detail. A surface study of IS-2062 MS was carried out by exposing the specimen to 6 h of immersion in a 3 M HCl system without and with 1 mg/L of expired ESLD. Contact angle (CA) measurements were performed using a Goniometer to comprehend the formation of inhibitor protective films. A basic drop wettability analyzer called Goniometer model FM41 was utilized to ascertain the effective wetting properties of MS, and 1 mg/L of expired was used for this purpose.

3. Results and Discussion

3.1. Potentiodynamic Polarization

Potentiodynamic polarization was recorded for the IS-2062 MS electrode in 3 M HCl without and with 0.25 mg/L, 0.5 mg/L, 0.75 mg/L, and 1 mg/L of expired ESLD at room temperature (303 K), and is presented in Figure 2 and Table 1. It is shown that corrosion current (I_{corr}) values significantly reduce with the introduction of expired ESLD, leading to enhanced protection efficiency. The I_{corr} value is high in the bare system compared to the protected system (expired ESLD), which is due to the aggressive nature of the 3 M HCl solution on the surface of MS. The aggressiveness of 3 M HCl is lessened when an inhibitor is present and increases the effectiveness of protection. Therefore, when the concentration of the inhibitor rises, so does the efficiency of inhibition. This can also be attributed to the formation of an adherent invisible layer over the surface of MS [26]. The values of the anodic (β_a) and cathodic (β_c) Tafel slopes do not differ significantly. Further, only minor variations (less than 85 mV) in the corrosion potential (E_{corr}) were observed when compared with the bare solution. This finding confirms that expired ESLD belongs to the mixed mode corrosion inhibitor. This inhibits the processes of anodic and cathodic disintegration [27]. Generally, the materials with E_{corr} and lower I_{corr} values exhibit better corrosion resistance [28].

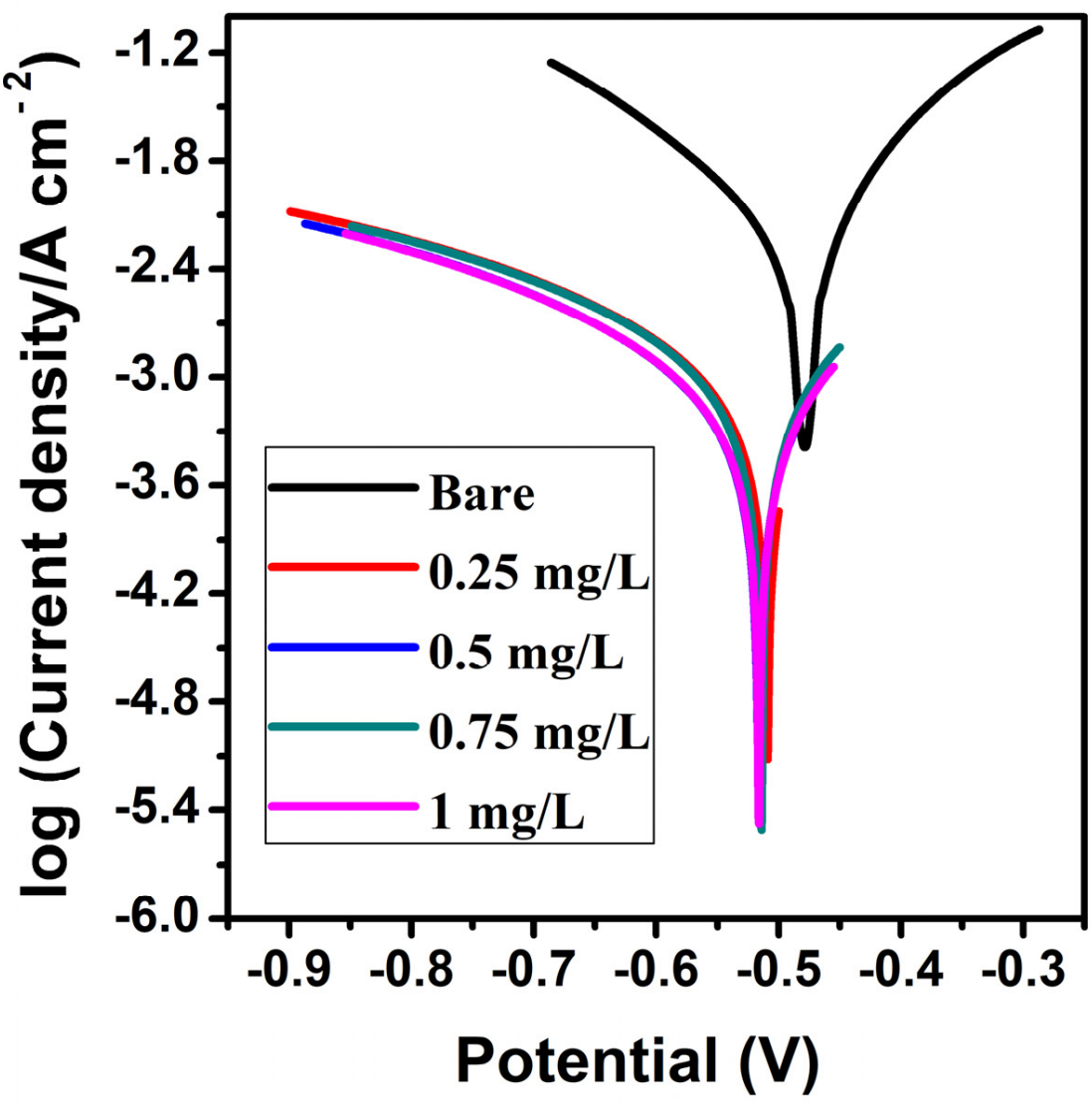


Figure 2. Tafel plots with and without an inhibitor for MS in 3 M HCl solution.

Table 1. Results of potentiodynamic polarization for MS in an acidic environment at ambient temperature.

Concentration (mg/L)	Corrosion Potential (mV)	Cathodic Tafel Slope (V/dec)	Anodic Tafel Slope (V/dec)	Corrosion Current (A)	Protection Efficiency
Bare	−483	−5.81	7.34	0.0071340	-
0.25	−510	−4.70	5.34	0.0005198	92.75
0.5	−517	−4.97	5.17	0.0003460	95.38
0.75	−515	−4.68	5.02	0.0003050	95.77
1.00	−518	−4.93	5.54	0.0002312	96.81

3.2. AC Impedance Spectroscopy

In the current investigation, AC impedance spectroscopy was used to control the electrochemical nature of MS in a 3 M HCl system. Figure 3 displays the Nyquist plots on the MS surface in a 3 M HCl system with and without an inhibitor of an expired ESLD.

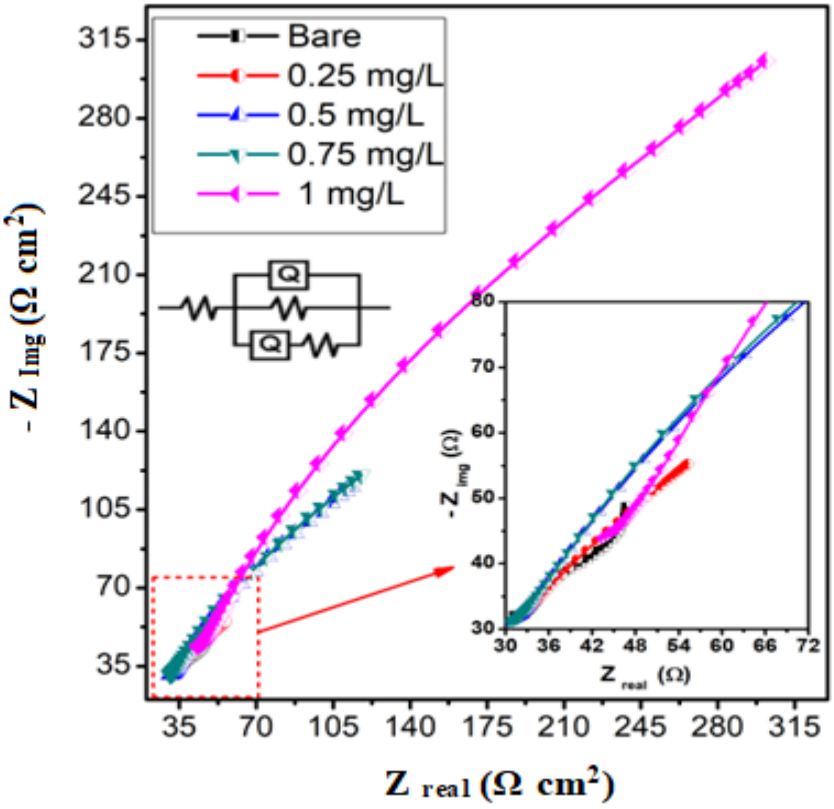


Figure 3. Nyquist curves for the MS exposed to the blank solution and acidic electrolytes with four distinct expired ESLD concentrations and equivalent circuits used in the present investigation (Figure 3).

Nearly semi-circular Nyquist plots show the process of charge transfer at the electrode/electrolyte interface [29]. Nyquist curves show imperfect single depressed capacitive loops with nearly identical shapes in the presence and absence of inhibitors, suggesting that the corrosion mechanism remains unchanged [30].

It is evident that the charge transfer resistance has increased as the inhibitor concentration has increased up to 1 mg/L, indicating the adsorption of inhibitor molecules on the metal surface. However, by substituting inhibitory spices for water molecules, the addition of the inhibitor to the test solution thickens the double layer and lowers the dielectric constant. In fact, the creation of a protective coating due to inhibitor molecules adhering to a metal surface has raised the charge transfer resistance [31–33].

The AC impedance results can be simulated on an equivalent circuit (Figure 3) to obtain more precise electrochemical parameters. Table 2 displays the findings from the Nyquist plots. The charge transfer resistance (R_{ct}) values rise when expired ESLD medication is added. This phenomenon was more obvious as the expired ESL drug concentration increased. The charge transfer resistance values rise as the concentration of expired ESLD increases, slowing the metal rate of disintegration and boosting protection effectiveness. In total, 1 mg/L of expired ESLD showed a maximum protection efficiency of 90%. As the concentration of expired ESLD increases, the diameter of the Nyquist curves gets larger. This shows that the introduction of expired ESLD strengthens the corrosion barrier layer on the 3 M HCl system. The Chi-squared values clearly show that the impedance data were best fitted to the proposed circuit.

Table 2. Results of electrochemical studies without and with inhibitor for MS in acidic electrolyte.

Concentration (mg/L)	Chi-Squared Value	Charge Transfer Resistance (Ω)	Protection Efficiency
Bare	1.35×10^{-5}	31.34	-
0.25	1.76×10^{-5}	49.93	37.23
0.5	2.54×10^{-5}	115.4	72.84
0.75	3.68×10^{-5}	141	77.77
1	2.07×10^{-5}	333.4	90.59

3.3. Gasometric Results

Gasometric studies were used to investigate the effects of four different concentrations of expired ESLD and contact time on the surface of MS in the 3 M HCl system at 303 K. The findings are displayed in Figure 4 and Table 3.

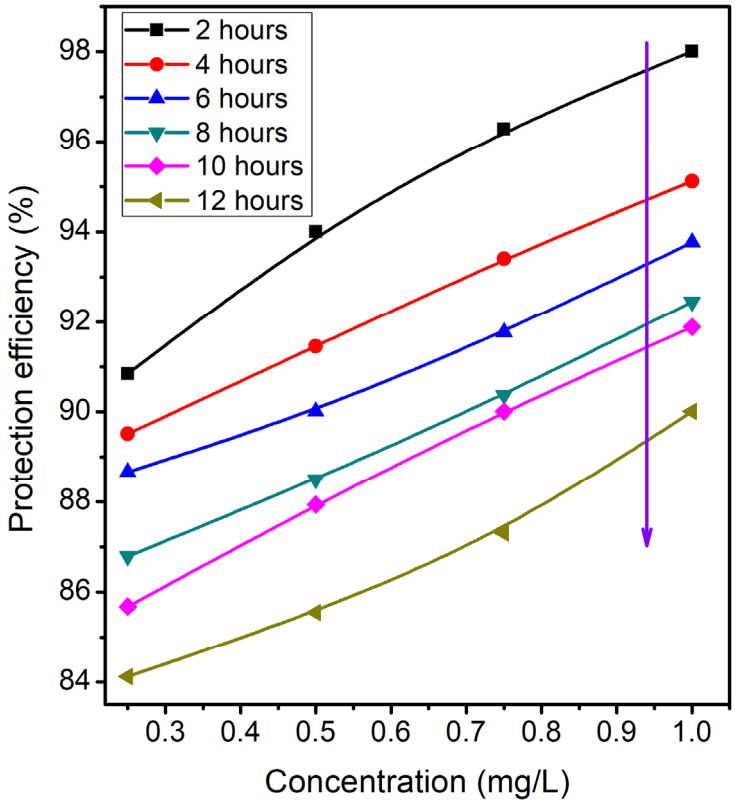


Figure 4. The relationship between the concentration of inhibitor and protection efficiency at different exposure periods.

Table 3. Gasometric results at different immersion periods, with protection efficiency repeated three times.

Immersion Time (hours)	Concentration (mg/L)	Volume of Hydrogen Gas Evolution (mL)	Surface Coverage (θ)	Protection Efficiency (%)
2	Bare	35	-	-
	0.25	3.2	0.908	90.85 ± 0.045%
	0.5	2.1	0.940	94.00 ± 0.032%
	0.75	1.3	0.962	96.28 ± 0.043%
	1	0.7	0.980	98.01 ± 0.016%
4	Bare	41	-	-
	0.25	4.3	0.895	89.51 ± 0.053%
	0.5	3.5	0.914	91.46 ± 0.067%
	0.75	2.7	0.934	93.41 ± 0.087%
	1	2.0	0.951	95.12 ± 0.035%
6	Bare	45	-	-
	0.25	5.1	0.886	88.66 ± 0.036%
	0.5	4.5	0.900	90.01 ± 0.038%
	0.75	3.7	0.917	91.77 ± 0.034%
	1	2.8	0.937	93.77 ± 0.024%
8	Bare	53	-	-
	0.25	7	0.867	86.79 ± 0.033%
	0.5	6.1	0.884	88.49 ± 0.037%
	0.75	5.1	0.903	90.37 ± 0.054%
	1	4	0.924	92.45 ± 0.058%
10	Bare	58	-	-
	0.25	8.3	0.856	85.68 ± 0.043%
	0.5	7	0.879	87.93 ± 0.063%
	0.75	5.8	0.900	90.01 ± 0.058%
	1	4.7	0.918	91.89 ± 0.047%
12	Bare	63	-	-
	0.25	10	0.841	84.12 ± 0.043%
	0.5	9.1	0.855	85.55 ± 0.038%
	0.75	8	0.873	87.30 ± 0.053%
	1	6.3	0.900	90.01 ± 0.048%

Similarly to the AC impedance and potentiodynamic polarization results, the corrosion inhibition efficiency of an expired ESLD is directly proportional to the inhibitor concentration. The adsorption of expired ESLD molecules on the MS surface in 3 M HCl solution is the cause of the increased protection efficiency. The water molecules that have been adsorbed will be replaced by the electron-rich components of the expired ESLD molecule that settle on the MS surface. As a result, the MS disintegration process is protected. Moreover, there exists an inverse relationship between the quantity of expired ESLD and the evolution of hydrogen gas. At 1 mg/L of expired ESLD, the highest protection efficiency and the lowest evolution of hydrogen gas were achieved. This significantly impedes the process of hydrogen evolution [25]. The immersion period has a negative effect on the protection efficiency of the expired ESLD.

3.4. Scanning Electron Microscopy (SEM) and Contact Angle (CA) Studies

The SEM technique was used to examine the surface morphology of MS in inhibited (1 mg/L of expired ESLD) and uninhibited aggressive solution with an immersion period of 4 h. The corresponding SEM results are shown in Figure 5. It is observed that the MS surface is greatly damaged with a rough structure without the addition of expired ESLD. In the presence of 1 mg/L of expired ESLD, the MS surface becomes uniform and smooth, and enlarged domain sizes in Figure 5b are proof of the passage of corrosive moieties

being blocked. This variation (from an uninhibited to inhibited system) fully confirms the protection efficiency of expired ESLD. The expired ESLD molecules undergo interaction with the MS surface and create a barrier layer which reduces the aggressive nature of the 3 M HCl solution on the MS surface.

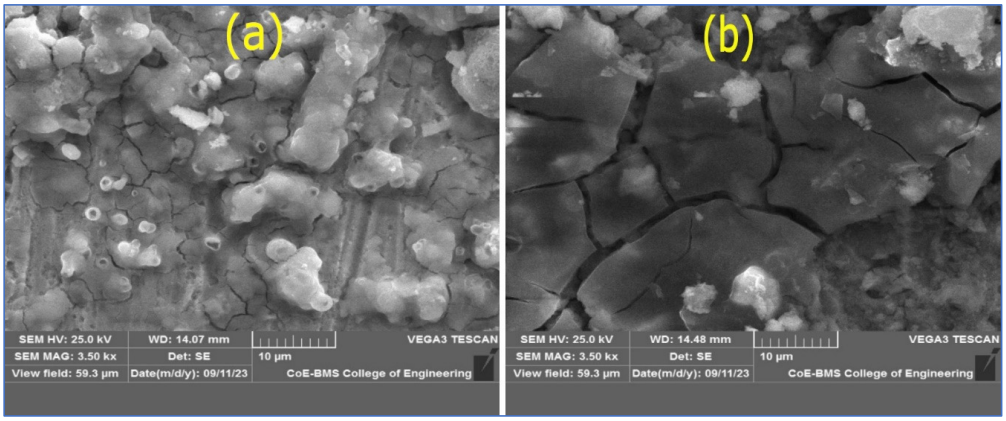


Figure 5. SEM images of (**a**) without and (**b**) with 1 mg/L of expired ESL drug at room temperature.

In corrosion studies, contact angle measurements are a useful tool for evaluating the wettability, behavior, and surface characteristics of materials in corrosive environments. When a droplet of corrosive solution is placed on the MS surface, it displays the interaction between the liquid and the surface. A hydrophilic surface has a contact angle of less than 90°, which indicates a strong affinity between the liquid and the solid surface, according to literature studies. A hydrophobic surface, on the other hand, has a contact angle of greater than 90° and tends to bead up rather than spread, indicating a low affinity between the liquid and the solid surface [34,35]. The contact angle of about 61° for MS dipped in HCl acid is displayed in Figure 6a. This shows that the corrosion process has altered the MS surface, resulting in a highly uneven corroded surface and a smaller contact angle. A higher contact angle of about 80° is seen in Figure 6b, indicating the formation of passive layers by the adsorbed species and the efficacy of the corrosion protection film. Higher contact angles are frequently preferred for corrosion resistance. In general, a greater water contact angle indicated an increased level of surface hydrophobicity [25]. The improvement in surface quality and the modification of material surface properties by the inhibitor is indicated by the increase in the contact angle before and after the addition of the indicator.

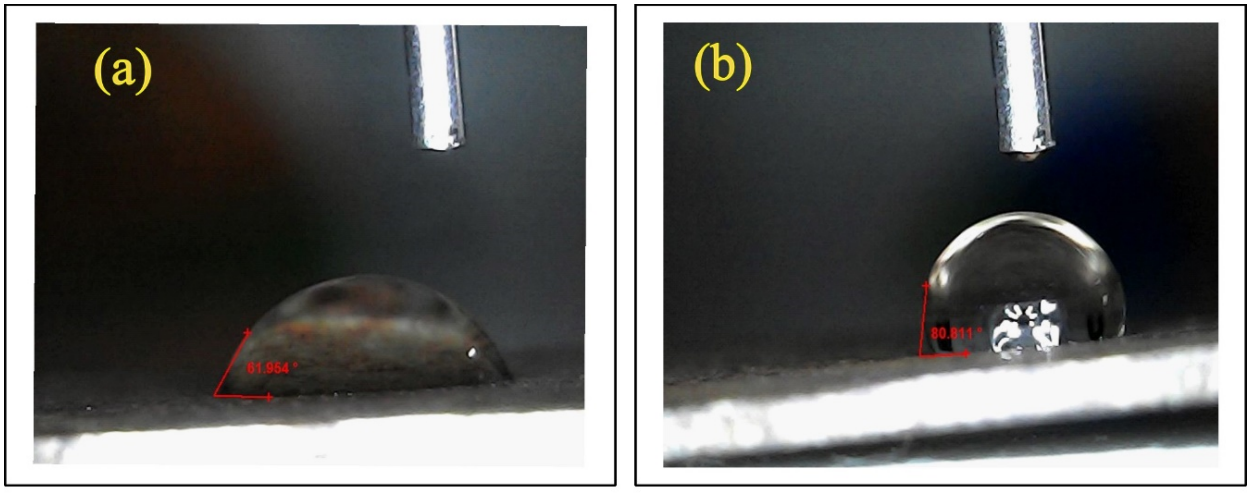


Figure 6. Water contact angle measurement. (**a**) Bare and (**b**) inhibited system.

3.5. Computational Studies

A broad picture of the spatial distribution of electron density, which could affect the molecules' reactivity, can be obtained by visually inspecting the molecular orbitals. In an aqueous system, theoretical investigations were conducted to screen the expired ESLD corrosion inhibition property on the MS. For this purpose, the DFT approach was used. The quantum chemical study results are shown in Figure 7 and Table 4. The high E_{HOMO} fully supports the electron donation property of expired ESLD on the surface of MS in a 3 M HCl system, and this generates an invisible barrier layer. This blocks the aggressive nature of the 3 M HCl system. The lower E_{LUMO} reveals the strong tendency to accept the electrons. In the current investigation, the results confirm that expired ESLD has an strong tendency to donate electrons to the MS surface in a 3 M HCl system. Although global reactivity descriptors provide useful information about the possible effectiveness of corrosion inhibitors, they frequently fall short of capturing the intricacy of the real inhibition mechanisms.

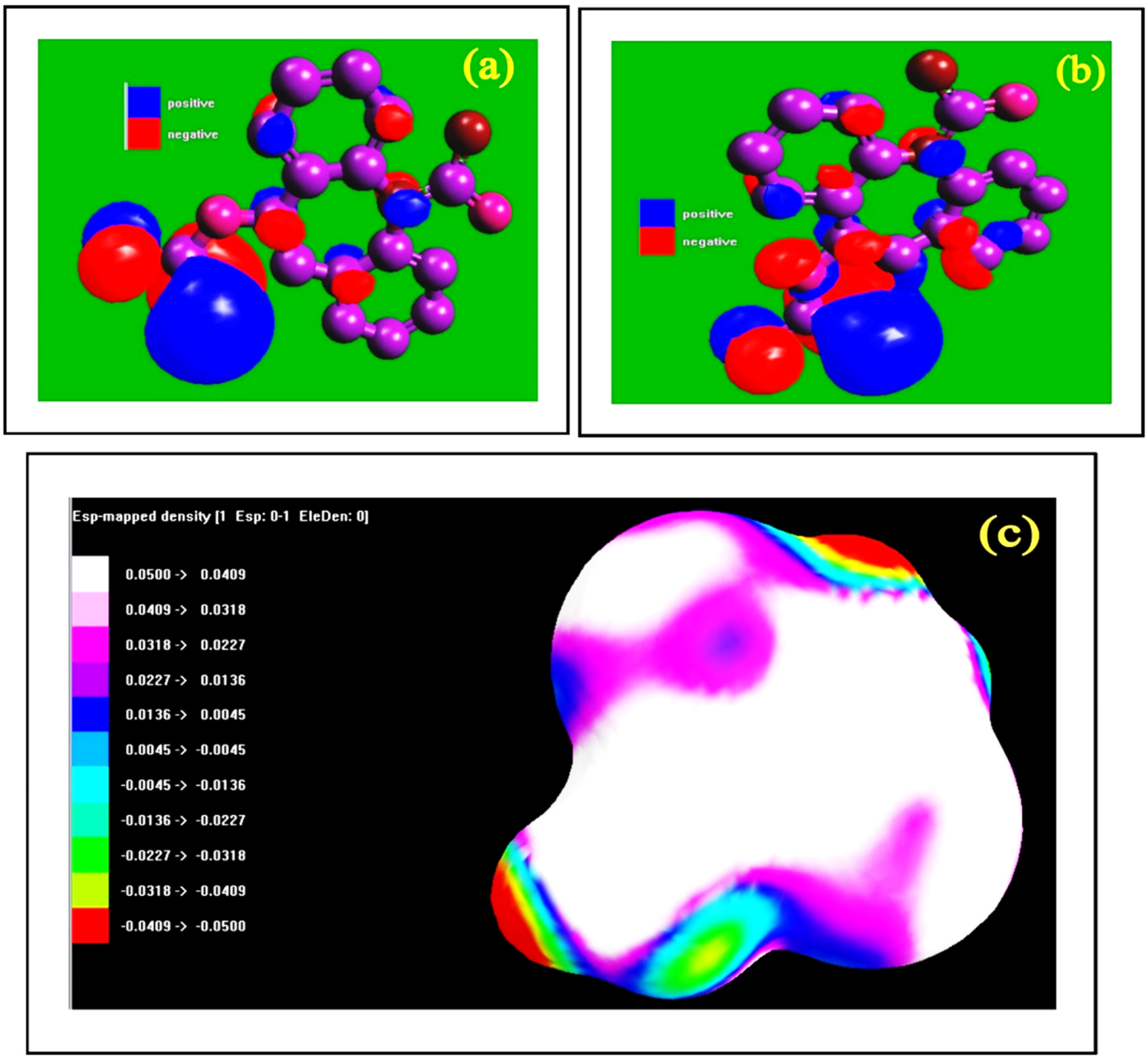


Figure 7. DFT results: (**a**) HOMO, (**b**) LUMO, and (**c**) density mapping of an expired drug.

Table 4. Quantum chemical results of expired ESL drug.

E_{HOMO} (eV)	E_{LUMO} (eV)	Energy Gap (eV)	I	A	η	χ	σ	μ	Ω
−11.029	−4.203	6.826	11.029	4.203	3.413	7.616	0.2929	−7.616	8.497

Further, the energy gap, electron affinity (A), ionization potential (I), chemical hardness (η), chemical softness (σ), electrophilicity index (ω), electronegativity (χ), and dipole moment (μ) fully back up the expired ESLD's ability to inhibit corrosion. Similar observations were reported in the literature [36,37]. The electron density results explain the location in the organic compound in which electron density is almost the same. The surface color indicates the polarity and magnitude of electrostatic potential [38].

Monte Carlo (MC) simulation was used to analyze the interaction between the Fe (1 1 0)/H_2O and expired ESLD molecule. The most stable configuration for drug adsorption from expired ESLD at the interface Fe (1 1 0)/H_2O is shown in Figure 8. Because of the high electron density of the expired ESL drug, the molecule aligns parallel to the Fe surface in this conformation, maximizing contact to increase surface coverage. Table 5 displays data indicating that expired ESLD molecules have higher adsorption energy than water molecules. An exceptionally high negative adsorption energy leads to stronger bonding to the Fe surface and the formation of a stable barrier film that effectively lowers MS corrosion. This finding supports the high inhibition efficiency observed in experimental studies and validates the role of expired drugs as a highly effective inhibitor against MS corrosion in environments containing 3 M HCl [39–41]. Figure 9 illustrates the schematic depiction of expired ESLD adsorption on the iron surface. As per the figure, the ESLD molecules positioned themselves on the Fe surface in an aqueous environment and blocked the surface against corrosive moieties in acidic solution. Such a molecular scheme may deepen our understanding of the role of ESLD as an anticorrosive agent. Overall, the results of the experimental studies are in good agreement with the DFT and MC simulation studies.

Table 5. MC simulation results in kcal/mol.

Total Energy	Adsorption Energy	Rigid Adsorption Energy	Deformation Energy	dE_{ad}/dN_I (ESL)	dE_{ad}/dN_I (Water)
−151.09	-3.23×10^5	−264.26	-3.23×10^5	-9.82×10^4	-4.51×10^4

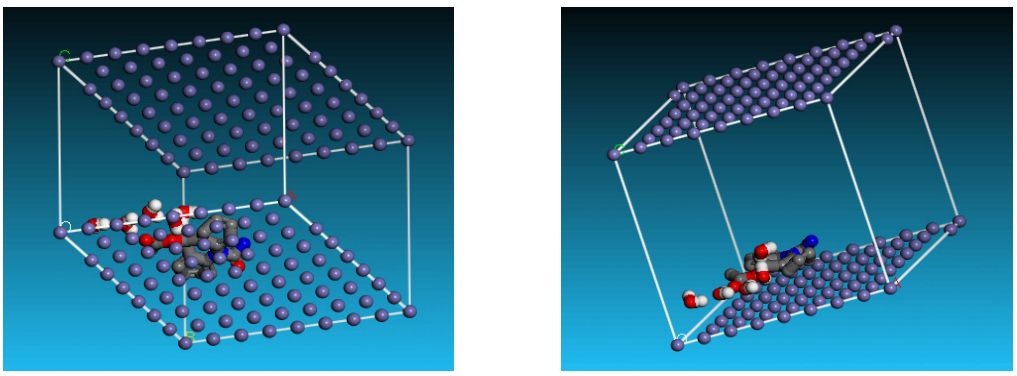


Figure 8. *Cont.*

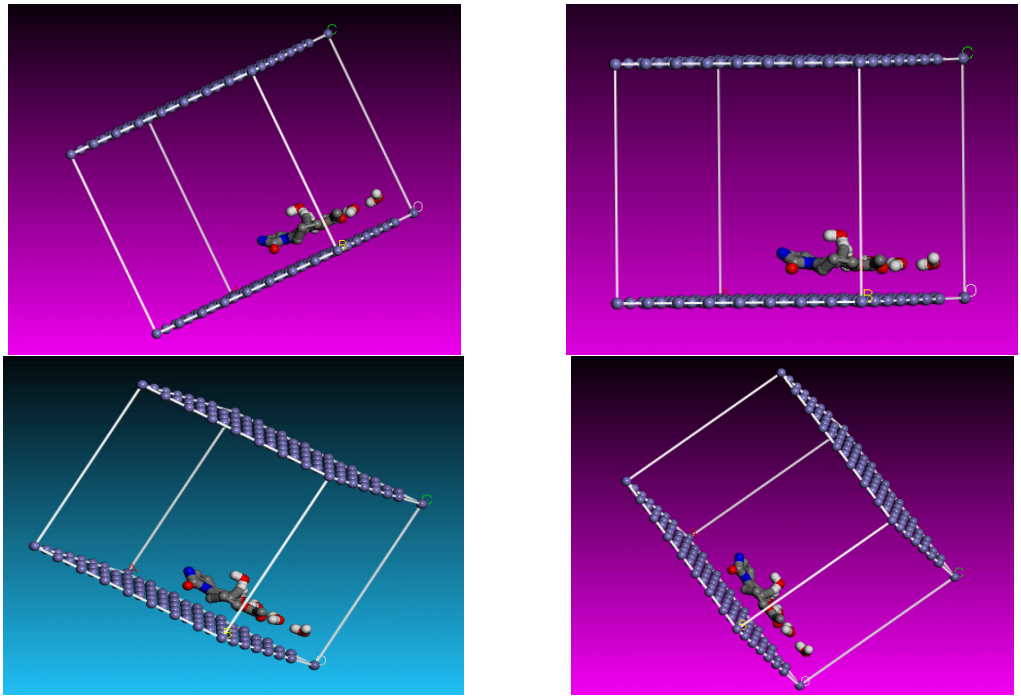


Figure 8. Images of the different views of the adsorption of expired ESLD molecules on the Fe surface in an aqueous environment.

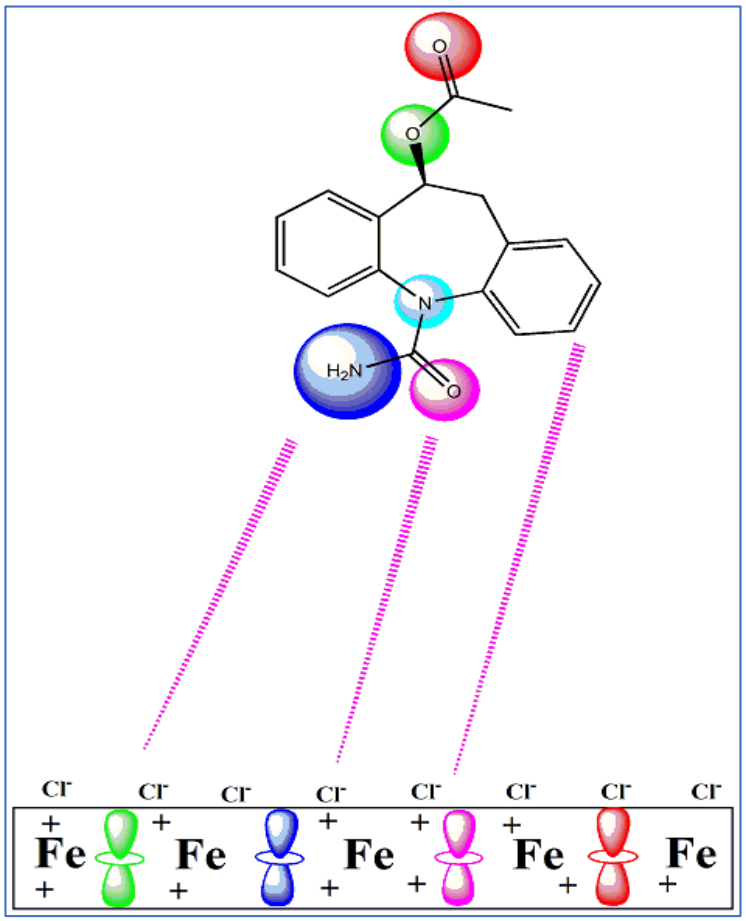


Figure 9. Diagram interpretation of the adsorption of expired ESLD on MS in acidic environments.

4. Conclusions

Through theoretical and experimental analyses, the corrosion-inhibiting efficacy of ESLD was systematically investigated. ESLD was applied as a sustainable anticorrosive substance to enhance corrosion protection against MS in a 3 M HCl solution. According to gasometric data, there is little evolution of hydrogen gas in the presence of expired ESLD. As the concentration of expired ESLD rises, protection effectiveness rises as well. Poptentiodynamic polarization (Tafel plots) showed that the expired ESLD mixed corrosion inhibition property on the MS in a 3 M HCl solution. The results of AC impedance spectroscopy indicate that as the concentration of expired ESLD rises, so does the charge transfer resistance. The expired ESLD was clearly detected within the SEM micrographs, demonstrating a smooth MS surface. In comparison with the bare system, the protected system has a higher contact angle. Both DFT and MC simulation supported interpretations in terms of the presence of strong interactions at the interface of the expired ESLD and the Fe (1 1 0) surface in an aqueous solution, which was in line with the experimental results. This approach can be considered in view of its environmental protection merit, besides providing the user with a functional green and environmentally safe material.

Author Contributions: Conceptualization, N.R., S.C. and M.R.S.; methodology, N.R., M.M.V. and M.R.S.; software, S.C.; validation, S.C., M.P. and M.R.S.; formal analysis, N.R., S.C., M.M.V., M.P. and M.R.S.; investigation, N.R., S.C., M.M.V., M.P. and M.R.S.; resources, N.R., S.C. and M.M.V.; data curation, N.R., S.C., M.M.V., M.P. and M.R.S.; writing—original draft preparation, N.R. S.C., M.M.V., M.P. and M.R.S.; writing—review and editing, M.P. and M.R.S.; visualization, N.R., S.C. and M.M.V.; supervision, M.R.S.; project administration, M.R.S. and M.P.; funding acquisition, M.P. All authors have read and agreed to the published version of the manuscript.

Funding: This research was funded from the statutory activities of Gdynia Maritime University, grant number WN/2025/PZ/14.

Data Availability Statement: The data are available on request.

Conflicts of Interest: The authors declare no conflicts of interest.

References

1. Bejandi, M.S.; Behroozi, M.H.; Khalili, M.R.; Sharifi, R.; Javidparvar, A.A.; Oguzie, E. Pharmaceuticals for materials protection: Experimental and computational studies of expired closantel drug ($C_{22}H_{14}C_{l2}I2N_2O_2$) as a potent corrosion inhibitor. *J. Ind. Eng. Chem.* **2023**, *131*, 662–675. [CrossRef]
2. Belhadj, N.; Maizia, R. Effectiveness of expired estradiol valerate drug molecule as a corrosion inhibitor for mild steel in 1 M HCl medium: Waste utilization perspective. *J. Indian Chem. Soc.* **2024**, *101*, 101287. [CrossRef]
3. Yadav, M.; Sinha, R.R.; Sarkar, T.K.; Tiwari, N. Corrosion inhibition effect of pyrazole derivatives on mild steel in hydrochloric acid solution. *J. Adhes. Sci. Technol.* **2015**, *29*, 1690–1713. [CrossRef]
4. Bhawsar, J.; Jani, M.; Jain, P. Evaluating the corrosion inhibition potential of expired ivermectin drug on mild steel: A comprehensive multi-method investigation. *Corros. Commun.* **2024**. [CrossRef]
5. Zakeri, A.; Zakeri, A.; Bahmani, E.; Bahmani, E.; Aghdam, A.S.R.; Aghdam, A.S.R. Plant extracts as sustainable and green corrosion inhibitors for protection of ferrous metals in corrosive media: A mini review. *Corros. Commun.* **2022**, *5*, 25–38. [CrossRef]
6. Mamudu, U.; Santos, J.H.; Umoren, S.A.; Alnarabiji, M.S.; Lim, R.C. Investigations of corrosion inhibition of ethanolic extract of Dillenia suffruticosa leaves as a green corrosion inhibitor of mild steel in hydrochloric acid medium. *Corros. Commun.* **2024**, *15*, 52–62. [CrossRef]
7. Bairagi, H.; Vashishth, P.; Ji, G.; Shukla, S.K.; Ebenso, E.E.; Mangla, B. Polymers and their composites for corrosion inhibition application: Development, advancement, and future scope–A critical review. *Corros. Commun.* **2024**, *15*, 79–94. [CrossRef]
8. Li, P.; Shao, Z.; Fu, W.; Ma, W.; Yang, K.; Zhou, H.; Gao, M. Enhancing corrosion resistance of magnesium alloys via combining green chicory extracts and metal cations as organic-inorganic composite inhibitor. *Corros. Commun.* **2023**, *9*, 44–56. [CrossRef]
9. Qiang, Y.; Guo, L.; Li, H.; Lan, X. Fabrication of environmentally friendly Losartan potassium film for corrosion inhibition of mild steel in HCl medium. *Chem. Eng. J.* **2020**, *406*, 126863. [CrossRef]

10. Mahdavian, M.; Tehrani-Bagha, A.R.; Alibakhshi, E.; Ashhari, S.; Palimi, M.J.; Farashi, S.; Javadian, S.; Ektefa, F. Corrosion of mild steel in hydrochloric acid solution in the presence of two cationic gemini surfactants with and without hydroxyl substituted spacers. *Corros. Sci.* **2018**, *137*, 62–75. [CrossRef]
11. El-Lateef, H.M.A. Experimental and computational investigation on the corrosion inhibition characteristics of mild steel by some novel synthesized imines in hydrochloric acid solutions. *Corros. Sci.* **2015**, *92*, 104–117. [CrossRef]
12. Jaiswal, M.; Saxena, A.; Kaur, J. Application of expired Febuxostat drug as an effective corrosion inhibitor for steel in acidic medium: Experimental and theoretical studies. *Chem. Data Collect.* **2024**, *52*, 101149. [CrossRef]
13. Oukhrib, R.; Abdellaoui, Y.; Berisha, A.; Oualid, H.A.; Halili, J.; Jusufi, K.; El Had, M.A.; Bourzi, H.; El Issami, S.; Asmary, F.A.; et al. DFT, Monte Carlo and molecular dynamics simulations for the prediction of corrosion inhibition efficiency of novel pyrazolylnucleosides on Cu(111) surface in acidic media. *Sci. Rep.* **2021**, *11*, 3771. [CrossRef] [PubMed]
14. Kasprzhitskii, A.; Lazorenko, G. Corrosion inhibition properties of small peptides: DFT and Monte Carlo simulation studies. *J. Mol. Liq.* **2021**, *331*, 115782. [CrossRef]
15. Ye, Y.; Yang, D.; Chen, H. A green and effective corrosion inhibitor of functionalized carbon dots. *J. Mater. Sci. Technol.* **2019**, *35*, 2243–2253. [CrossRef]
16. Lei, G.; Lei, Z.; Chin-Hung, L.; Bochuan, T.; Jun, C.; Riadh, M.; Yan, T.; Amir Mahmoud, M. Mango leaves extract as sustainable corrosion inhibitor for X70 steel in HCl medium: Integrated experimental analysis and computational electronic/atomic-scale simulation. *Sustain. Mater. Techno.* **2024**, *42*, e01167. [CrossRef]
17. Sheetal; Thakur, S.; Singh, A.K. Corrosion inhibition of mild steel by expired pyridoxine hydrochloride in 0.5 M H_2SO_4 solution. *Inorg. Chem. Commun.* **2024**, *166*, 112602. [CrossRef]
18. Qiang, Y.; Zhang, S.; Tan, B.; Chen, S. Evaluation of Ginkgo leaf extract as an eco-friendly corrosion inhibitor of X70 steel in HCl solution. *Corros. Sci.* **2018**, *133*, 6–16. [CrossRef]
19. Abdallah, M. Antibacterial drugs as corrosion inhibitors for corrosion of aluminium in hydrochloric solution. *Corros. Sci.* **2003**, *46*, 1981–1996. [CrossRef]
20. Sundaram, R.G.; Vengatesh, G.; Sundaravadivelu, M. Surface morphological and quantum chemical studies of some expired drug molecules as potential corrosion inhibitors for mild steel in chloride medium. *Surf. Interfaces* **2020**, *22*, 100841. [CrossRef]
21. Wiśniewska, P.; Saeb, M.R.; Bencherif, S.A. Biomaterials recycling: A promising pathway to sustainability. *Front. Biomater. Sci.* **2023**, *2*, 1260402. [CrossRef]
22. Vaszilcsin, N.; Kellenberger, A.; Dan, M.L.; Duca, D.A.; Ordodi, V.L. Efficiency of Expired Drugs Used as Corrosion Inhibitors: A Review. *Materials* **2023**, *16*, 5555. [CrossRef] [PubMed]
23. Attia, E.; Hyba, A.; Attia, E.M.; Hassan, N.S.; Hyba, A.M. Potentiodynamic Study on the Effect of Expired Septazole and Septrin Drugs on the Corrosion Inhibition of Tin Electrode in 1 M HCl Solution. *J. Basic. Appl. Chem.* **2019**, *9*, 11–18.
24. Raghavendra, N.; Bhat, J.I. Chemical components of mature areca nut husk extract as a potential corrosion inhibitor for mild steel and copper in both acid and alkali media. *Chem. Eng. Commun.* **2017**, *205*, 145–160. [CrossRef]
25. Raghavendra, N. Expired naproxen drug as a robust corrosion inhibitor of Al in 3 M hydrochloric acid system. *Songklanakarin J. Sci. Technol.* **2020**, *42*, 917–922. [CrossRef]
26. Kalaiselvi, P.; Chellammal, S.; Palanichamy, S.; Subramanian, G. Artemisia pallens as corrosion inhibitor for mild steel in HCl medium. *Mater. Chem. Phys.* **2010**, *120*, 643–648. [CrossRef]
27. Ma, X.; Jiang, X.; Xia, S.; Shan, M.; Li, X.; Yu, L.; Tang, Q. New corrosion inhibitor acrylamide methyl ether for mild steel in 1 M HCl. *Appl. Surf. Sci.* **2016**, *371*, 248–257. [CrossRef]
28. Sathishkumar, A.; Soundararajan, R.; Sivasankaran, S.; Ramesh, A. Influence of eutectic-Si in as-cast and fibrous-eutectic-Si in LPBF-processed $AlSi_{10}Mg$ alloys on wear and corrosion behaviors treated with direct aging route. *J. Mater. Sci.* **2023**, *58*, 14889–14910. [CrossRef]
29. Ahamad, I.; Prasad, R.; Quraishi, M. Thermodynamic, electrochemical and quantum chemical investigation of some Schiff bases as corrosion inhibitors for mild steel in hydrochloric acid solutions. *Corros. Sci.* **2009**, *52*, 933–942. [CrossRef]
30. Aslam, R.; Mobin, M.; Aslam, J.; Lgaz, H.; Chung, I.-M. Inhibitory Effect of Sodium Carboxymethylcellulose and Synergistic Biodegradable Gemini Surfactants as Effective Inhibitors for MS Corrosion in 1 M HCl. *J. Mater. Res. Technol.* **2019**, *8*, 4521–4533. [CrossRef]
31. Chitra, S.; Parameswari, K.; Selvaraj, A. Dianiline Schiff bases as inhibitors of mild steel corrosion in acid media. *Int. J. Electrochem. Sci.* **2023**, *5*, 1675–1697. [CrossRef]
32. Solmaz, R. Investigation of corrosion inhibition mechanism and stability of Vitamin B1 on mild steel in 0.5 M HCl solution. *Corros. Sci.* **2014**, *81*, 75–84. [CrossRef]
33. Popoola, L.T. Progress on pharmaceutical drugs, plant extracts and ionic liquids as corrosion inhibitors. *Heliyon* **2019**, *5*, e01143. [CrossRef] [PubMed]

34. Behera, P.K.; Rao, S.; Popoola, L.T.; Swamirayachar, S.A.; AlFalah, M.G.K.; Kandemirli, F.; Kodange, S.; Prashanth, G.K.; Achalkumar, A.S. Room Temperature Columnar Liquid Crystalline Perylene Bisimide as a Novel Corrosion Resistant Surface Film for Mild Steel Surface. *J. Bio- Tribo-Corros.* **2022**, *9*, 18. [CrossRef]
35. Renuka, P.; Rao, S.; Rao, P.; S, S.S.; Prashanth, G. Corrosion mitigation of mild steel in 1 M HCl acid using an expired drug: An experimental approach. *Inorg. Chem. Commun.* **2023**, *160*, 111871. [CrossRef]
36. Wang, W.; Qu, F.; Zhang, Y.; Liu, Z.; Chang, H.; Xia, L.; Kong, M.; Lv, Y.; Li, G. Enhanced corrosion resistance of flaky carbonyl iron through dual silane surface modification for the application of electromagnetic wave absorption coatings. *J. Mater. Sci.* **2024**, *59*, 1721–1735. [CrossRef]
37. Raghavendra, N. Expired Lorazepam Drug: A Medicinal Compound as Green Corrosion Inhibitor for Mild Steel in Hydrochloric Acid System. *Chem. Afr.* **2019**, *2*, 463–470. [CrossRef]
38. Abeng, F.E.; Anadebe, V.C. Combined electrochemical, DFT/MD-simulation and hybrid machine learning based on ANN-ANFIS models for prediction of doxorubicin drug as corrosion inhibitor for mild steel in 0.5 M H_2SO_4 solution. *Comput. Theor. Chem.* **2023**, *1229*, 114334. [CrossRef]
39. Benzbiria, N.; Thoume, A.; El Caid, Z.A.; Echihi, S.; Elmakssoudi, A.; Zarrouk, A.; Zertoubi, M. An investigation on the utilization of a synthesized benzodiazepine derivative as a corrosion inhibitor for carbon steel in sulfuric solution: Chemical and electrochemical synthesis, surface analysis (SEM/AFM), DFT and MC simulation. *Colloids Surf. A Physicochem. Eng. Asp.* **2023**, *681*, 132744. [CrossRef]
40. Elqars, E.; Laamari, Y.; Sadik, K.; Bimoussa, A.; Oubella, A.; Mechnou, I.; Auhmani, A.; Taha, M.L.; Essadki, A.; Aboulmouhajir, A.; et al. Synthesis, experimental, theoretical, and molecular dynamic studies of 1-(2,5-dimethoxy-4-methylphenyl)ethan-1-thiosemicarbazone as green inhibitor for carbon steel corrosion. *J. Mol. Struct.* **2023**, *1282*, 135228. [CrossRef]
41. Barrodi, M.R.; Mirzaee, A.; Kafashan, A.; Zahedifard, S.; Majidi, H.J.; Davoodi, A.; Hosseinpour, S. Synergistic effect in Tragacanth Gum-Ceftriaxone hybrid system as an environmentally friendly corrosion inhibitor for mild steel in acidic solutions. *Mater. Today Commun.* **2023**, *34*, 105390. [CrossRef]

Disclaimer/Publisher's Note: The statements, opinions and data contained in all publications are solely those of the individual author(s) and contributor(s) and not of MDPI and/or the editor(s). MDPI and/or the editor(s) disclaim responsibility for any injury to people or property resulting from any ideas, methods, instructions or products referred to in the content.